Charmless B Decays at Belle II

Sagar Hazra

Tata Institute of Fundamental Research,

Mumbai 400 005, India

E-mail: sagar.hazra@tifr.res.in

We report the measurements of *CP* asymmetry and branching fraction of various charmless B decays at the Belle II experiment. We use a $62.8\,\text{fb}^{-1}$ sample of electron-positron collisions collected at the $\Upsilon(4S)$ resonance. All the results agree with previous determinations and establish good performance of the Belle II detector.

11th International Workshop on the CKM Unitarity Triangle (CKM2021)
November 22–26, 2021
The University of Melbourne, Australia

1. Introduction

The study of charmless B decays is a keystone of the flavor physics program to test the standard model (SM) and its extension. These decays are mediated by Cabbibo-suppressed $b \to u$ tree and $b \to d, s$ loop transitions, and provide sensitive probes to non-SM contributions. The CKM angle $\alpha/\phi_2 \equiv arg(-\frac{V_{td}V_{tb}^*}{V_{ud}V_{ub}^*})$ can be measured directly only by an analysis of charmless $B \to \pi\pi, \rho\rho$ decays related by isospin symmetry. Isospin symmetry is also used to build sum-rules, i.e. linear combination of branching fractions and CP asymmetries of charmless decays, that can provide SM null tests with precision generally better than 1%. Belle II has the unique capability of studying jointly, and within a consistent experimental environment, all relevant final states of isospin-related B decays to improve the knowledge of alpha and to put stringent bound on sum-rule tests.

Belle II [2] is a magnetic spectrometer having almost 4π solid-angle coverage, designed to reconstruct final-state particles of e^+e^- collisions delivered by the SuperKEKB asymmetric-energy collider [3], located at the KEK laboratory in Tsukuba, Japan. The Belle II experiment started collecting data from March 2019. In this proceeding, we will focus on the result based on a dataset corresponding to an integrated luminosity of $62.8\,\mathrm{fb}^{-1}$ which has been collected at the $\Upsilon(4S)$ resonance.

2. Analysis overview and Challenges

We form final-state particle candidate by applying loose baseline selection criteria and then combine them in kinematic fits consistent with the topologies of the desired decays to reconstruct intermediate states and B candidates. The key challenge in reconstructing significant charmless signal is the large contamination from $e^+e^- \to q\overline{q}$ ($q = u, d, s, c$) continuum background coupled with low signal branching fraction. We use a binary-decision-tree classifier that combines a number of mostly topological variables having some discrimination between B-meson signal and continuum background. We pick up those variables whose correlation with ΔE and M_{bc} is below $\pm 5\%$ to reduce possible bias in the signal yield determination. The latter two are the energy difference $\Delta E = E_B^* - \sqrt{s}/2$ between the energy of the reconstructed B candidate and half of the collision energy, both in the $\Upsilon(4S)$ frame, and the beam-energy-constrained mass $M_{\mathrm{bc}} = \sqrt{s/(4c^4) - (p_B^*/c)^2}$, which is the invariant mass of the B candidate with its energy being replaced by the half of the center-of-mass collision energy. Another challenge is to separate B background events that peak in the signal region. To deal with this peaking background, we either kinematically veto it from the sample or include a separate component in the fit model. For example, in the analysis of $B \to K\pi\pi$ decays the background from $B^+ \to \overline{D}^0(\to K^+\pi^-)\pi^+$ decays is suppressed by vetoing candidates with a kaon-pion mass in the range $[1.84, 1.89]$ GeV/c^2. We then apply optimized continuum suppression and particle identification criteria. To determine signal efficiency and to develop fit models, we use simulation and correct or validate it with control data. To determine the systematic uncertainties, pseudo-experiment and control channel studies are performed. We developed and tested the full analysis with simulated events and control sideband data (i.e. region where signal is not expected) before inspecting the most interesting region (or, signal region) on data to measure the physics observables.

3. Isospin sum-rule

The isospin sum-rule relation for the $B \to K\pi$ system provides a stringent test of the SM [1],

$$I_{K\pi} = \mathcal{A}_{K^+\pi^-} + \mathcal{A}_{K^0\pi^+} \frac{\mathcal{B}(K^0\pi^+)}{\mathcal{B}(K^+\pi^-)} \frac{\tau_{B^0}}{\tau_{B^+}} - 2\mathcal{A}_{K^+\pi^0} \frac{\mathcal{B}(K^+\pi^0)}{\mathcal{B}(K^+\pi^-)} \frac{\tau_{B^0}}{\tau_{B^+}} - 2\mathcal{A}_{K^0\pi^0} \frac{\mathcal{B}(K^0\pi^0)}{\mathcal{B}(K^+\pi^-)} = 0, \quad (1)$$

where $\mathcal{B}$, $\mathcal{A}$ and τ are the branching fraction, direct CP asymmetries and lifetime of B decays, respectively. In all the four $K\pi$ channels, signal yields are determined with unbinned extended maximum-likelihood fits of the ΔE and $M_{\rm bc}$ distributions. We measure the time-integrated asymmetry of the CP-eigenstate $B^0 \to K^0\pi^0$ by inferring the B meson flavor q from that of the other B-meson produced on the $\Upsilon(4S)$ decay, using by the category-based flavor tagger [4]. The asymmetry $\mathcal{A}_{K^0\pi^0}$ is determined from a simultaneous maximum-likelihood fit to the unbinned $M_{\rm bc}$–ΔE–$q \cdot r$ distributions, where r is the dilution factor of flavor tagger output that accounts for wrongly tagged events. The signal probability density function (PDF) is given by

$$\mathcal{P}_{\rm sig} = \frac{1}{2}(1 + q \cdot r \cdot (1 - 2\chi_d)\mathcal{A}_{K^0\pi^0}), \quad (2)$$

where χ_d is the B^0–$\bar{B}^0$ mixing frequency. Figures 1 and 2 show the ΔE distribution of all the four $K\pi$ system. We obtain the following branching fractions,

$$\begin{aligned}
\mathcal{B}(B^0 \to K^+\pi^-) &= [18.0 \pm 0.9(\text{stat}) \pm 0.9(\text{syst})] \times 10^{-6}, \\
\mathcal{B}(B^+ \to K^+\pi^0) &= [11.9^{+1.1}_{-1.0}(\text{stat}) \pm 1.6(\text{syst})] \times 10^{-6}, \\
\mathcal{B}(B^+ \to K^0\pi^+) &= [21.4^{+2.3}_{-2.2}(\text{stat}) \pm 1.6(\text{syst})] \times 10^{-6}, \\
\mathcal{B}(B^0 \to K^0\pi^0) &= [8.5^{+1.7}_{-1.6}(\text{stat}) \pm 1.2(\text{syst})] \times 10^{-6}
\end{aligned}$$

and CP-violating rate asymmetries

$$\begin{aligned}
\mathcal{A}_{CP}(B^0 \to K^+\pi^-) &= -0.16 \pm 0.05(\text{stat}) \pm 0.01(\text{syst}), \\
\mathcal{A}_{CP}(B^+ \to K^+\pi^0) &= -0.09 \pm 0.09(\text{stat}) \pm 0.03(\text{syst}), \\
\mathcal{A}_{CP}(B^+ \to K^0\pi^+) &= -0.01 \pm 0.08(\text{stat}) \pm 0.05(\text{syst}), \\
\mathcal{A}_{CP}(B^0 \to K^0\pi^0) &= -0.40^{+0.46}_{-0.44}(\text{stat}) \pm 0.04(\text{syst}).
\end{aligned}$$

The dominant contribution in the systematic uncertainties comes from the π^0 and K_S^0 reconstruction efficiency for the decays having this final state particles. These are determined in the control sample of data and are expected to significantly reduced with larger sample size.

4. *CP* violation in multibody decays

The study of multibody charmless B decays has recently attracted significant attention [5]. The contribution between weak- and strong-interaction dynamics in $B^+ \to K^+K^-K^+$, $B^+ \to K^+\pi^-\pi^+$ and $B^0 \to K^+\pi^-\pi^0$ decays are enriched by the amplitude structure accessible via their Dalitz plot. In Fig. 3 we show the ΔE distributions for two of these multibody systems. We obtain the following
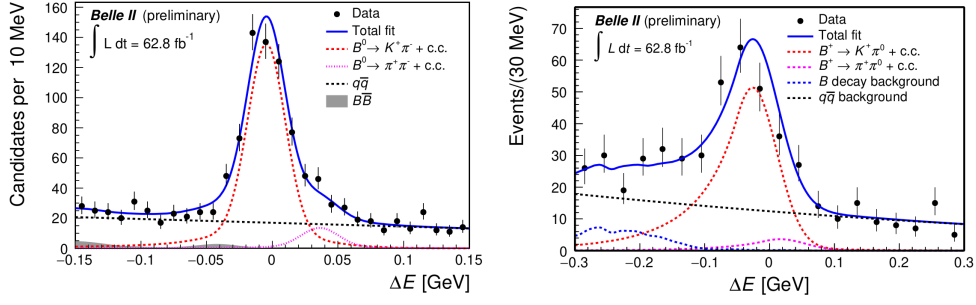
3

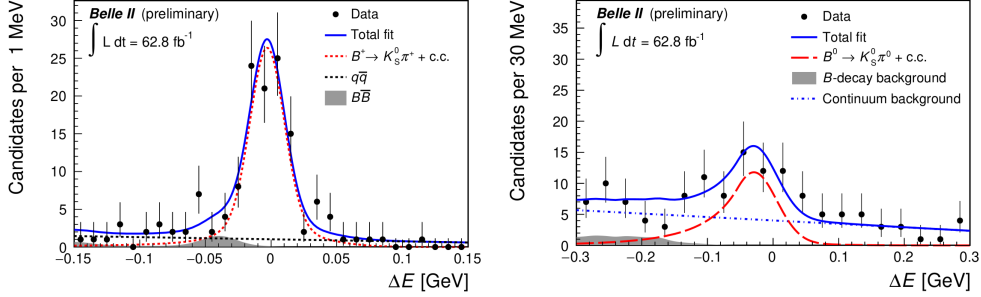**Figure 1:** Signal-enhanced ΔE distributions of $B^0 \to K^+\pi^-$ (left) and $B^+ \to K^+\pi^0$ (right).

Figure 2: Signal-enhanced ΔE distributions of $B^+ \to K^0\pi^+$ (left) and $B^0 \to K^0\pi^0$ (right).

branching fractions,

$$
\begin{aligned}
\mathcal{B}(B^+ \to K^+K^-K^+) &= [35.8 \pm 1.6(\text{stat}) \pm 1.4(\text{syst})] \times 10^{-6}, \\
\mathcal{B}(B^+ \to K^+\pi^-\pi^+) &= [67.0 \pm 3.3(\text{stat}) \pm 2.3(\text{syst})] \times 10^{-6}, \\
\mathcal{B}(B^0 \to K^+\pi^-\pi^0) &= [38.1 \pm 3.5(\text{stat}) \pm 3.9(\text{syst})] \times 10^{-6}
\end{aligned}
$$

and *CP*-violating rate asymmetries

$$
\begin{aligned}
\mathcal{A}_{CP}(B^+ \to K^+K^-K^+) &= -0.103 \pm 0.042(\text{stat}) \pm 0.020(\text{syst}), \\
\mathcal{A}_{CP}(B^+ \to K^+\pi^-\pi^+) &= -0.010 \pm 0.050(\text{stat}) \pm 0.021(\text{syst}), \\
\mathcal{A}_{CP}(B^0 \to K^+\pi^-\pi^0) &= +0.207 \pm 0.088(\text{stat}) \pm 0.011(\text{syst}).
\end{aligned}
$$

Also in this case, the largest systematic uncertainties comes from π^0 reconstruction for $B^0 \to K^+\pi^-\pi^0$. For the others, the dominant systematic uncertainties is the tracking efficiency, which will also be reduced with more data.

5. Towards the determination of α/ϕ_2

The combined analysis of branching fractions and *CP* violating asymmetries of the complete set of $B \to \pi\pi$, $\rho\rho$ isospin partners enables a determination of α [6]. We focus here on $B^0 \to \pi^0\pi^0$, $B^+ \to \pi^+\pi^0$, $B^0 \to \pi^+\pi^-$ and $B^+ \to \rho^+\rho^0$ decays. The $B^0 \to \pi^0\pi^0$ channel is particularly challenging as it requires the reconstruction of two $\pi^0 \to \gamma\gamma$ decays. A dedicated boosted-decision-trees classifier used to suppress background photons by combining 20 calorimetric variables. Signal
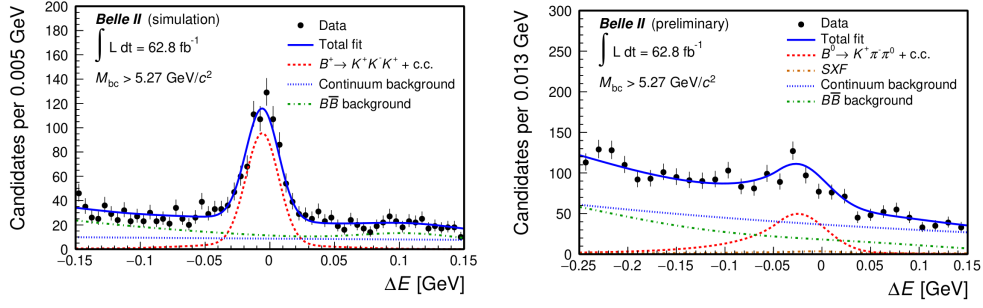
Figure 3: Signal-enhanced ΔE distributions of $B^+ \rightarrow K^+ K^- K^+$ (left) and $B^0 \rightarrow K^+ \pi^- \pi^0$ (right).

yields are determined with an extended maximum-likelihood fit of the ΔE, M_{bc} and transformed continuum suppression variable. Figure 4 shows the ΔE distribution of two $\pi\pi$ channels. We obtain the following branching fractions,

$$\mathcal{B}(B^0 \rightarrow \pi^+ \pi^-) = [5.8 \pm 0.7(\text{stat}) \pm 0.7(\text{syst})] \times 10^{-6},$$
$$\mathcal{B}(B^+ \rightarrow \pi^+ \pi^0) = [5.5^{+1.0}_{-0.9}(\text{stat}) \pm 0.7(\text{syst})] \times 10^{-6},$$
$$\mathcal{B}(B^0 \rightarrow \pi^0 \pi^0) = [0.98^{+0.48}_{-0.39}(\text{stat}) \pm 0.27(\text{syst})] \times 10^{-6}$$

and CP asymmetry of $\mathcal{A}_{CP}(B^+ \rightarrow \pi^+ \pi^0) = -0.04 \pm 0.17(\text{stat}) \pm 0.06(\text{syst})$. The $B^+ \rightarrow \rho^+ \rho^0$ decay involves pion-only final state, where the large width of the $m(\rho)$ mesons offers reduced distinctive features against dominant continuum background. Isolating a low-background signal is therefore the main challenge of the analysis. Signal yields are determined with an unbinned maximum-likelihood fits of ΔE, continuum-suppression decision-tree output, the dipion masses and cosines of helicity angles of the ρ candidates. Figure 5 shows the ΔE and $m(\pi^+ \pi^-)$ of $B^+ \rightarrow \rho^+ \rho^0$ candidates. We obtain the branching fraction $\mathcal{B} = [20.6 \pm 3.2(\text{stat}) \pm 4.0(\text{syst})] \times 10^{-6}$ and longitudinal polarization fraction $f_L = 0.936^{+0.049}_{-0.041}(\text{stat}) \pm 0.021(\text{syst})$. The dominant contribution in the systematic uncertainties comes from π^0 reconstruction and tracking efficiency.
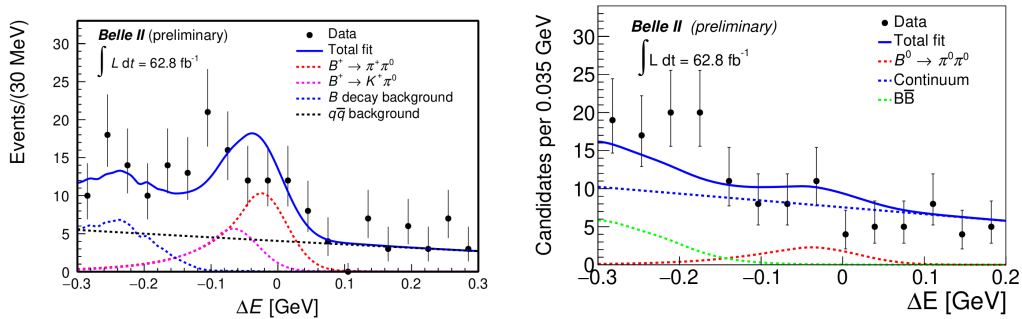

Figure 4: Signal-enhanced ΔE distributions of $B^+ \rightarrow \pi^+ \pi^0$ (left) and $B^0 \rightarrow \pi^0 \pi^0$ (right).
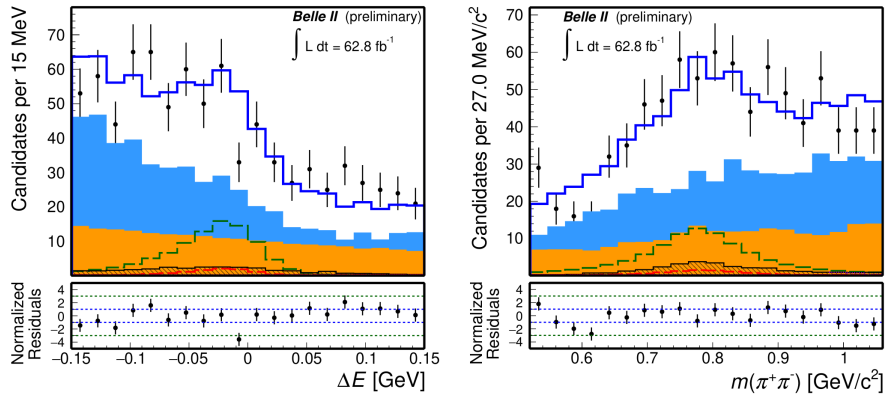
Figure 5: Distributions of ΔE (left) and $m(\pi^+\pi^-)$ (right) for $B^+ \to \rho^+\rho^0$ candidates.

6. Summary

Charmless B decays play an important role in sharpening the flavor picture. Belle II is getting ready to play a lead role in testing isospin sum rules, in the study of CP violation in multibody decays, and in the determination of α. We presented the preliminary measurements of charmless decays performed using a sample of early data corresponding to an integrated luminosity of $62.8\,\mathrm{fb}^{-1}$. First Belle II measurement of $B^0 \to K^0\pi^0$ completes the ingredients for the isospin sum rule; $B \to \rho\rho$ and $\pi\pi$ analysis show performance comparable to Belle result. All results agree with known values within uncertainties and are mostly limited by the current small sample size.

References

[1] M. Gronau, Phys. Lett. B **627**, 82 (2005).

[2] T. Abe et al. (Belle II Collaboration), arXiv:1011.0352.

[3] K. Akai et al. (SuperKEKB Group), Nucl. Instrum. Meth. A **907**, 188 (2018).

[4] F. Abudinén et al. (Belle II Collaboration), arXiv:2110.00790

[5] R. Aaij et al. , LHCb Collaboration, Phys. Rev. Lett. **112** (2014) 011801.

[6] M. Gronau and D. London, Phys. Rev. Lett. **65** (1990) 3381.